



Single Crystalline Germanium-Lead Alloy on Germanium Substrate Formed by Pulsed Laser Epitaxy

Qian Zhou,^a Taw Kuei Chan,^b Sin Leng Lim,^b Chunlei Zhan,^a Thomas Osipowicz,^b Xiao Gong,^a Eng Soon Tok,^b and Yee-Chia Yeo^{a,z}

^aDepartment of Electrical and Computer Engineering, National University of Singapore (NUS), Singapore

^bDepartment of Physics, National University of Singapore (NUS), Singapore

Single crystalline germanium-lead alloy (GePb) is synthesized for the first time using pulsed laser induced epitaxy. Amorphous GePb with Pb content of 3% was deposited on Ge substrate and followed by pulsed laser annealing. Two sets of laser fluence, 300 mJ/cm² and 400 mJ/cm², were used in this work. The as-grown GePb alloy has good crystalline quality, as confirmed by transmission electron microscopy. No dislocation or Pb precipitation is found in the GePb layer. High-resolution Rutherford Backscattering Spectrometry (HRBS) characterization indicates that substitutional Pb content in the GePb alloy is 0.2 ± 0.1%. There is a substantial loss of Pb atoms after GePb formation according to the HRBS results. More serious Pb outdiffusion is observed for the sample annealed at 400 mJ/cm² than that annealed at 300 mJ/cm².

© 2014 The Electrochemical Society. [DOI: 10.1149/2.0141407ssl] All rights reserved.

Manuscript submitted April 4, 2014; revised manuscript received May 12, 2014. Published May 29, 2014.

Silicon-germanium, as a group IV material alloy, has been widely used in semiconductor devices. Other group IV alloys, e.g. silicon-carbon¹ and germanium-tin,² have also gain research attention in recent years. However, there are not many reports on the alloy of germanium and lead (GePb) so far. The study of GePb mainly focused on the basic material properties, e.g. equilibrium phase diagram,³ dissociation energy,⁴ and intermetallic bond.⁵ One experimental report on GePb is about the electrical properties as a function of Pb mole fraction.⁶ Recently, there is a report claiming that GePb could be a direct bandgap material for substitutional Pb concentration less than 1%.⁷ This provides strong motivation for the formation of single crystalline GePb with Pb atoms in the substitutional sites, since a group-IV direct bandgap material can enable the integration of laser components to the Si platform.^{8,9} However, the atomic radius difference between Ge and Pb is very large (23.2%), and this makes it difficult to form a single crystalline GePb epitaxial layer on Ge substrate. In a previous study,⁶ the GePb alloy was formed by evaporation of the constituents from Ge and Pb targets, and amorphous GePb (α -GePb) alloy was obtained. There is no report of epitaxial growth of single crystalline GePb so far. Whether Pb atoms can be incorporated in the substitutional sites of the Ge lattice is still unknown.

In this paper, single crystalline GePb alloy with substitutional Pb was formed on a Ge substrate by pulsed laser induced epitaxy. It is known that laser can induce a non-equilibrium recrystallization process,¹⁰⁻¹³ and that the laser anneal can activate dopants well above the maximum solid solubility limit.¹⁴⁻¹⁷ A non-equilibrium process employing pulsed laser anneal was utilized to form GePb alloy in this work. Good crystalline quality was observed using Transmission Electron Microscopy (TEM). High-resolution Rutherford Backscattering Spectrometry (HRBS) results show that Pb atoms was successfully incorporated in the substitutional sites of the Ge lattice, and the content of substitution Pb atoms is 0.2 ± 0.1 at%. The effect of laser fluence to the GePb formation is also studied. Higher laser fluence leads to stronger Pb outdiffusion according to the conventional RBS measurement. On the other hand, the HRBS results indicate that a higher laser fluence may lead to a higher substitutional Pb concentration.

The process steps for forming single crystalline GePb alloy are as follows. An n-type Ge wafer with (100) orientation was used as the starting substrate. Following cleaning by diluted HF solution (HF:H₂O = 1:100) for 3 minutes, a 30-nm-thick amorphous GePb layer was deposited by magnetron sputtering system at a pressure of 5 × 10⁻⁶ Torr. The GePb target used for sputtering is a mixture of Ge and Pb (Ge:Pb = 97:3). The sputtering was carried out at room temperature, and the DC power applied for the target is 200 W. The estimated GePb layer thickness is ~30 nm. After the deposition of GePb, 15 nm of SiO₂ was deposited on the GePb surface without breaking vacuum.

Since the laser annealing is not performed in vacuum or inert gas ambient, the GePb could be oxidized during the annealing if there is no capping layer on it. The role of SiO₂ is to protect GePb surface from oxidation. After the sputtering process, pulsed KrF excimer laser was employed to crystallize the amorphous GePb layer. The wavelength of the KrF laser is 248 nm, and pulse duration is ~23 ns. Two sets of laser fluence, 300 mJ/cm² and 400 mJ/cm², were used for GePb alloy formation. During the annealing, the laser beam with a beam spot size of 3 × 3 mm² scanned through the entire sample surface. Each spot was irradiated by 5 times and the overlap between two beam spots was 5 μm. It should be noted that the laser fluence mentioned above (300 mJ/cm² or 400 mJ/cm²) refers to the fluence of a single pulse.

A TEM image of the as-deposited GePb is shown in Fig. 1a. The interface between Ge (100) substrate and amorphous GePb layer is clearly observed. The thickness of GePb is ~30 nm, which agrees with the expected value based on sputtering process conditions. Fig. 1b illustrates the cross-sectional view of GePb layer after 300 mJ/cm² laser annealing, and Fig. 1c is the high magnification view of a location near the GePb surface. From the TEM images, it is confirmed that the GePb layer was crystallized after laser annealing. The local high temperature induced by pulsed laser leads to an epitaxial growth of GePb layer. The as-deposited GePb could melt during laser annealing and then epitaxially grow from the Ge substrate. There is no dislocation at the interface between GePb and Ge [Fig. 1b], and no Pb precipitate or cluster was observed in the GePb film [Fig. 1c], indicating that a good GePb crystalline quality can be obtained using the laser induced epitaxy.

To quantify the total Pb concentration and the substitutional Pb content, both the conventional RBS and HRBS characterization were

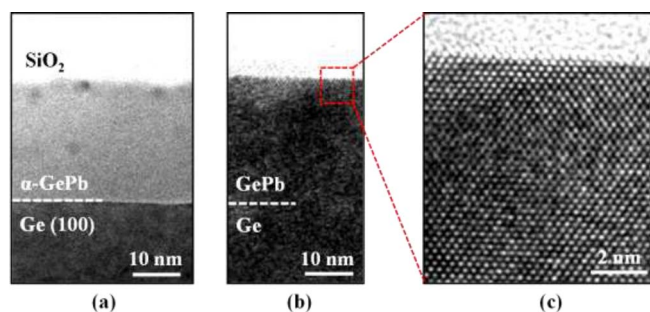


Figure 1. (a) Cross-sectional TEM image of as-deposited GePb sample (30 nm). The GePb is amorphous after deposition. (b) The GePb layer is recrystallized after laser annealing. Good epitaxial quality of GePb on Ge substrate is achieved. (c) Single crystalline GePb is observed in high magnification TEM image. No Pb precipitation or clustering was observed.

^zE-mail: yeo@iecc.org

carried out. The conventional RBS was used to determine the total number of Pb atoms, while the HRBS was used to get the percentage of substitutional Pb. In this work, it is important to know the percentage of substitutional Pb, since the band structure and electrical properties of the GePb alloy are more related to the substitutional Pb concentration.⁷

In the conventional RBS measurement, the incident beam (2 MeV He⁺ ions) was at normal incidence, with scattering angle of 150°. Passivated Implanted Planar Silicon (PIPS) detector with resolution of 17 keV was used to detect the signal. Since Pb atoms may diffuse into SiO₂ capping layer during laser anneal, the estimation of Pb content in GePb would be affected if the SiO₂ is capped on GePb in the RBS measurement. Thus, the SiO₂ layer was removed before the RBS measurement to ensure that the signal is collected from GePb layer. Fig. 2 shows the conventional RBS results of the samples annealed at 300 mJ/cm² and 400 mJ/cm². It is clearly observed that the Pb signal counts of the sample annealed at 400 mJ/cm² is much lower than that of the sample annealed at 300 mJ/cm², indicating a significant difference in total amount of Pb atoms between the two samples. The total amount of Pb (in atoms/cm²) can be estimated by curve fitting using SIMNRA. The extracted values are 7×10^{14} atoms/cm² and 2×10^{14} atoms/cm² for the samples annealed at 300 mJ/cm² and 400 mJ/cm², respectively. The use of a higher laser fluence could have caused a lower Pb dose incorporated in GePb. Since the local temperature during the 400 mJ/cm² anneal is higher

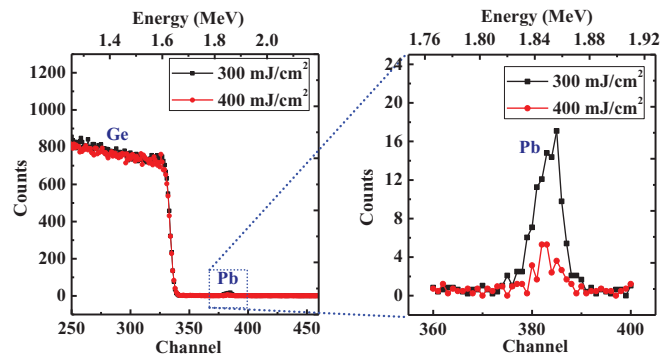


Figure 2. The conventional RBS results of the samples annealed using laser fluence of 300 mJ/cm² and 400 mJ/cm². The Pb signal counts of sample annealed at 400 mJ/cm² is much lower than that annealed at 300 mJ/cm², indicating a lower total Pb concentration in the samples annealed at 400 mJ/cm².

than that in the 300 mJ/cm² anneal, this could enhance the Pb atom outdiffusion and result in a lower Pb concentration in the GePb layer.

HRBS results for the samples annealed at 300 mJ/cm² and 400 mJ/cm² are shown in Fig. 3a and Fig. 3b, respectively. The SiO₂

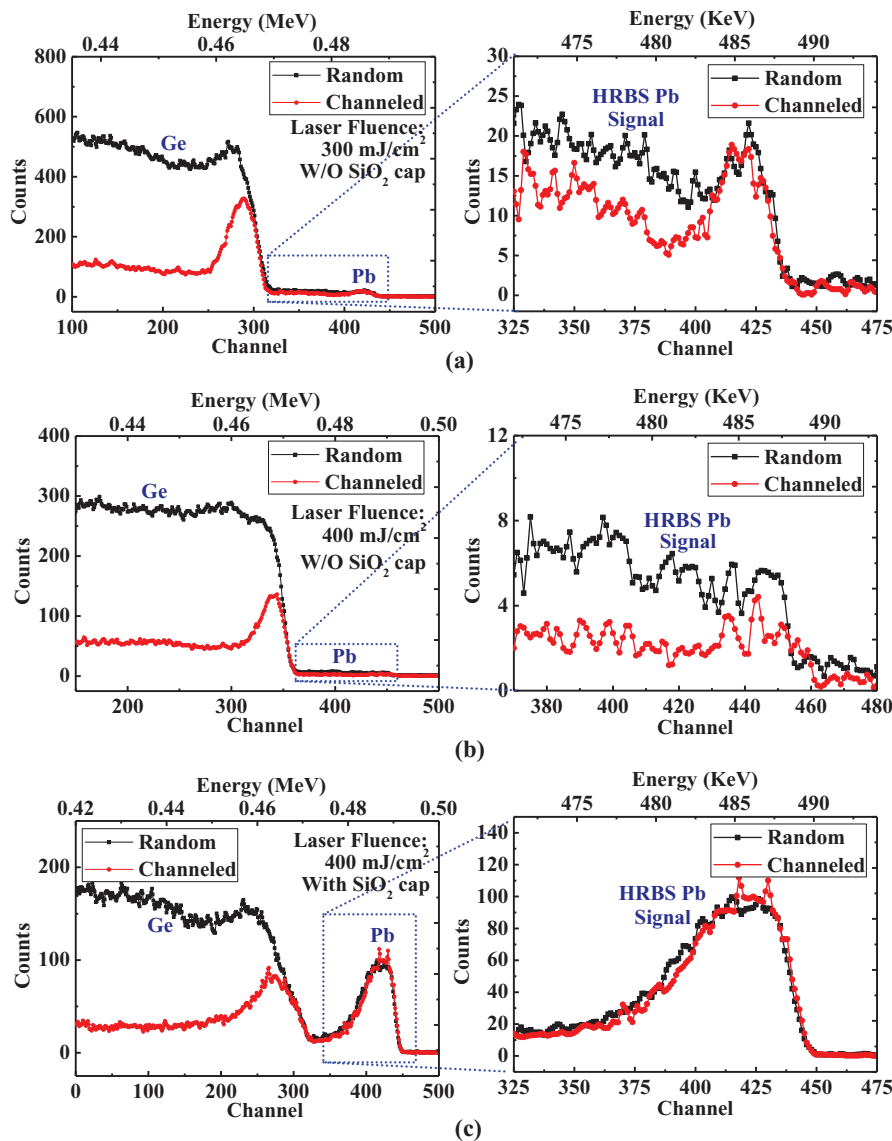


Figure 3. Random and channeled HRBS spectra of the samples after laser induced epitaxy. (a) Sample annealed using laser fluence of 300 mJ/cm². (b) Sample annealed using laser fluence of 400 mJ/cm². The Pb-rich SiO₂ capping layer was removed before HRBS measurement in (a) and (b). (c) Sample annealed at 400 mJ/cm² and the SiO₂ capping was not removed. It is estimated that the substitutional Pb content in the GePb alloy is $0.2 \pm 0.1\%$. The segregation of Pb atoms into the SiO₂ capping is confirmed by the HRBS measurement.

capping layer was also removed to ensure that the signal is collected from GePb layer. A spectrometer / focal plane detector with an energy resolution of about 1.5 keV was used in the HRBS system. The incident He⁺ ion energy is 500 keV and the scattering angle is 65°. More details of the HRBS setup can be found in ref. 18. Both the random and <111> aligned/channeled HRBS spectra are shown in Fig. 3a and Fig. 3b. High magnification spectra of Pb are also shown to illustrate the difference between random and aligned/channeled HRBS results. Curve fitting of random spectrum indicates that the total Pb contents in GePb layer are $0.5 \pm 0.1\%$ and $0.3 \pm 0.1\%$ for samples annealed at 300 mJ/cm² and 400 mJ/cm², respectively. This is consistent with the extracted value from the conventional RBS results, where higher laser fluence leads to smaller total Pb amount. It should be noted that the total Pb content estimated from HRBS results has an error range of $\pm 0.1\%$, and this is due to the weak Pb signal in the HRBS measurement. Since the Pb signal is comparable to the background signal level, it is difficult to get the accurate Pb contents by curve fitting. In this study, the main purpose of HRBS is to determine the percentage of substitutional Pb out of the total Pb amount. The substitutional Pb percentages are $\sim 47\%$ and $\sim 74\%$ in the samples annealed at 300 mJ/cm² and 400 mJ/cm², respectively. Combined with the total Pb content, one can deduce that the substitutional Pb content in the GePb alloy is $0.2 \pm 0.1\%$. Although the total Pb amount is smaller in the sample annealed at higher fluence, the percentage of substitutional Pb is larger. Fig. 3c shows the HRBS spectra for the 400 mJ/cm² annealed sample with SiO₂ capping layer. The counts of Pb signal are much higher than that of the sample without SiO₂ capping, and the channeled Pb signal is comparable to the random Pb signal. It is implied that there is a large amount of Pb atoms in the SiO₂ capping layer. Since PbO-SiO₂ has a wide glass formation composition range (up to 90 mol% PbO),¹⁹ high Pb concentration could be expected in the SiO₂ capping layer. Using a capping material which has a smaller Pb solubility would reduce the Pb outdiffusion and increase the Pb concentration in Ge substrate. Thus, higher substitutional Pb concentration may be obtained by combining a capping layer with low Pb solubility and high laser fluence.

In conclusion, single crystalline GePb alloy was successfully formed using sputtering and pulsed laser induced epitaxy. Two sets of laser fluence, 300 mJ/cm² and 400 mJ/cm², were used. This is the first demonstration of epitaxial growth of GePb alloy on Ge substrate. The GePb alloy shows a good crystalline quality without Pb precipitation or clustering. No dislocation is observed at the interface between GePb and Ge from TEM images. HRBS characterization indicates that the total Pb contents in GePb layer are $0.5 \pm 0.1\%$ and $0.3 \pm 0.1\%$ for

the samples annealed at 300 mJ/cm² and 400 mJ/cm², respectively. The sample annealed at higher laser fluence has more serious Pb outdiffusion. HRBS results also show that Pb atoms are successfully introduced in the substitutional sites. The content of substitutional Pb atoms is $0.2 \pm 0.1\%$.

Acknowledgment

This work was supported by Singapore National Research Foundation through the Competitive Research Program (Grant No: NRF-CRP6-2010-4).

References

1. K.-J. Chui, K.-W. Ang, N. Balasubramanian, M.-F. Li, G. Samudra, and Y.-C. Yeo, *IEEE Trans. Elect. Dev.*, **54**, 249 (2007).
2. X. Gong, G. Han, F. Bai, S. Su, P. Guo, Y. Yang, R. Cheng, D. Zhang, G. Zhang, C. Xue, B. Cheng, J. Pan, Z. Zhang, E. S. Tok, D. Antoniadis, and Y.-C. Yeo, *IEEE Elect. Dev. Lett.*, **34**, 339 (2013).
3. R. W. Olesinski and G. J. Abbaschian, *Bulletin of Alloy Phase Diagrams*, **5**, 374 (1984).
4. A. Ciccioli, G. Gigli, G. Meloni, and E. Testani, *J. Chem. Phys.*, **127**, 054303 (2007).
5. A. Ciccioli and G. Gigli, *The Open Thermodynamics Journal*, 7(Suppl 1: M8), 77 (2013).
6. G. Deutscher and M. L. Rappaport, *Le Journal de Physique – Letters*, **40**, 219 (1979).
7. W. Huang, B. Cheng, C. Xue, and C. Li, *Physica B*, (2014). In press.
8. A. A. Tonkikh, C. Eisenschmidt, V. G. Talalaev, N. D. Zakharov, and J. Schilling, *Appl. Phys. Lett.*, **103**, 032106 (2013).
9. G. Chang, W. Hsieh, J. Chen, and H. H. Cheng, *Opt. Lett.*, **38**, 3485 (2013).
10. J. S. Williams, W. L. Brown, H. J. Leamy, J. M. Poate, J. W. Rodgers, D. Rousseau, G. A. Rozgonyi, J. A. Shelnett, and T. T. Sheng, *Appl. Phys. Lett.*, **33**, 542 (1978).
11. J. R. Abelson, T. W. Sigmon, K. B. Kim, and K. H. Weiner, *Appl. Phys. Lett.*, **52**, 230 (1988).
12. K. J. Kramer, S. Taiwar, and T. W. Sigmon, *Appl. Phys. Lett.*, **61**, 769 (1992).
13. S.-M. Koh, X. Wang, K. Sekar, W. Krull, G. S. Samudra, and Y.-C. Yeo, *J. Electrochem. Society*, **156**, H361 (2009).
14. Geert Hellings, Erik Rosseel, Eddy Simoen, Dunja Radisic, Dirch Hjorth Petersen, Ole Hansen, Peter Folmer Nielsen, Gerd Zschätzsch, Aftab Nazir, Trudo Clarysse, Wilfried Vandervorst, Thomas Y. Hoffmann, and Kristin De Meyer, *Electrochem. Solid-State Lett.*, **14**, H39 (2011).
15. S. Heo, S. Baek, D. Lee, M. Hasan, H. Jung, J. Lee, and H. Hwang, *Electrochem. Solid-State Lett.*, **9**, G136 (2006).
16. Q. Zhang, J. Huang, N. Wu, G. Chen, M. Hong, L. K. Bera, and C. Zhu, *IEEE Elect. Dev. Lett.*, **27**, 728 (2006).
17. A. T. Koh, R. T.-P. Lee, F.-Y. Liu, T.-Y. Liow, K.-M. Tan, X. Wang, G. S. Samudra, D.-Z. Chi, N. Balasubramanian, and Y.-C. Yeo, *IEEE Elect. Dev. Lett.*, **29**, 464 (2008).
18. T. Osipowicz, H. L. Seng, T. K. Chan, and B. Ho, *Nucl. Instr. and Meth. in Phys. Res. B*, **249**, 915 (2006).
19. S. Kohara, H. Ohno, M. Takata, T. Usuki, H. Morita, K. Suzuya, J. Akola, and L. Pusztai, *Phys. Rev. B*, **82**, 134209 (2010).